

Numerical Optimization of Plasmonic Biosensors

Dominique Barchiesi

*GAMMA3 project (INRIA-UTT)- Charles Delaunay Institute - University of technology of
Troyes 12 rue Marie Curie - BP 2060 - 10010 TROYES cedex
France*

1. Introduction

Since the engineering control of the deposition of nanometric gold plates on substrates the Surface Plasmon Resonance (SPR) based sensor has become one of the most successful label-free and commercially developed optical sensor, with applications to biology (Hoaa et al., 2007; Kolomenskii et al., 1997; Kretschman & Raether, 1968; Lecaruyer et al., 2006). This technique is currently employed in biomolecular engineering, drug design, monoclonal antibody characterization, virus-protein interaction, environmental pollutants detection, among other interesting problems. The basic principle of such transducer is the measurement of the sudden absorption of light by the thin metallic layer, under particular illumination conditions (p-polarization) and a specific angle of incidence of the illumination (Barchiesi, Kremer, Mai & Grosgees, 2008; Barchiesi, Macías, Belmar-Letellier, Van Labeke, Lamy de la Chapelle, Toury, Kremer, Moreau & Grosgees, 2008; Kretschman & Raether, 1968), leading to a highly sensitive device (Kolomenskii et al., 1997; Lecaruyer et al., 2006). The conditions of such absorption are linked to the plasmon resonance in metallic structure, and therefore a tiny change of the optical properties of medium above the gold plate, produces an angular shift of this absorption, due to the detuning of the resonance. The sensing principle relies therefore on the shift of the plasmonic resonance caused by the surrounding dielectric environmental change in a binding event.

The Plasmonic biosensors use the property of resonance between an illumination and the metallic part of the sensor. This resonance is used to increase the sensitivity of the biosensor and the threshold of detection. Actually, a given set of parameters of the biosensor can lead to a maximum of the absorption of the incoming light. A slight change of its immediate environment (presence/Absence of biomolecules to be detected) produces a strong change of the detected light due to the detuning of the resonance. This property is also used in cancer therapy or imaging, through metallic nanoparticles or nanoshells (Grosgees, Barchiesi, Toury & Gréhan, 2008). The design of specific shapes for nanoparticles can help to tune the resonance for specific applications (Billot et al., 2006).

In the case of planar SPR (Surface Plasmon Resonance) biosensors, the reflected intensity vanishes for a specific angle of incidence. The illumination is almost totally coupled in the metal layer. A tiny change of the optical index of the upper medium, due to the presence of biomolecules, produces a measurable shift of this minimum. Therefore, to improve the efficiency of the sensor, the material and geometrical characteristics of the materials involved in the biosensor must be adjusted correctly. Surprisingly, the optimization of such structures has rarely been addressed (Ekgasit et al., 2005; Kolomenskii et al., 1997; Lecaruyer et al.,

2006) and only recently with metaheuristic methods (Barchiesi, Macías, Belmar-Letellier, Van Labeke, Lamy de la Chapelle, Toury, Kremer, Moreau & Grosge, 2008). Thus, the numerical optimization is becoming a useful tool, especially with the aim to apply to the optimization of nanostructured biosensors for which a large number of parameters has to be adjusted, making unapplicable a classical experimental design plan.

In this chapter, the requirements of such numerical optimization are put to the front, before introducing some optimization methods and discussing results. The first approach of optimization is based on deterministic methods, where a specific behavior of the bio-sensor is emphasized. For example, the influence of the thickness of the gold plate in SPR, all other parameters being fixed. More general methods of optimization are based on heuristics, and use the "random wizard," known to find what is hidden: the best parameters, much more efficiently than a systematic search, based on loops on each parameter. Among the various metaheuristic approaches, we focus on two specifics. Both are based on the bio-mimicry by numerical methods, by using life characteristics, stealing cross-over, mutation, selection, cooperation...

2. Optimization requirements: stand back and deepen the knowledge on the model

To get significant and reliable numerical results in numerical optimization, the most important requirement is having a realistic, efficient and numerically stable model. Even if this point seems to be obvious, this constraint on the model for its use for numerical optimization is not always fulfilled. Actually, numerical models entail *endogenous* (physically significant), and *exogenous* inputs. Among the exogenous parameters, some of them are linked to the mathematical model (the number of terms in series, the choice of scattering (S) or transmission (T) formulation (Li, 1994; 1996)...) and many are related to the numerical methods (the integration step size, the maximum degree of polynomials of interpolation, the stop criterion, the method of inversion, the discretization, the number of terms in series (Barchiesi et al., 2006; Barchiesi, Macías, Belmar-Letellier, Van Labeke, Lamy de la Chapelle, Toury, Kremer, Moreau & Grosge, 2008; Grosge et al., 2007; Grosge, Borouchaki & Barchiesi, 2008; Grosge et al., 2010; 2005)...))

If trends are considered as sufficient to compare experiments and numerical simulations, the exogenous inputs are often adjusted manually within the domain of physical (endogenous) parameters used for the model.

Instead, for optimization, the model is used as a black box, and the exogenous inputs must be adjusted automatically to produce stable and converged results. The model should be used blindly and remaining always reliable. This aspect of development of a stable numerical model is particularly critical in the case of resonance depiction, leading intrinsically to numerical instabilities. We encountered such a problem with FDTD (Macías et al., 2004), with evolutionary methods, the FDTD using regular Yee's cells for computation, like DDA used dipoles of the same size. This fact produced instabilities in the optimization, which prefers a continuity of the computed result with discretization. Indeed, the plasmon resonance can be described mathematically as the occurrence of a pole (in the complex plane) in the diffusion matrix, and this property has to be correctly handled. The two following sub-section illustrate two aspects of care to provide to the mathematical formulation.

2.1 The plasmon resonance and the model of biosensor

The SPR involves at least one metal layer, sometimes two, for improving the stick of the gold layer (Barchiesi, Macías, Belmar-Letellier, Van Labeke, Lamy de la Chapelle, Toury, Kremer,

Moreau & Grosge, 2008). The gold layer is the active part of the biosensor (Fig. 1). The incoming illumination is characterized by its p polarized electric field E_i (the magnetic field is parallel to the layer). The SPR biosensors use the Kretschmann configuration (Kretschmann, 1978), and therefore, the reflected (or specular) field intensity $R = |E_r|^2$ is detected. The transmitted field E_t is the probe of the biomolecules. Basically, a metal is highly reflecting. However, the launch of plasmon corresponds to the maximum of energy transfer from the illumination to the metal layer. The track of the plasmon resonance is therefore highlighted by the detection of the minimum of the reflected intensity $R(\theta)$.

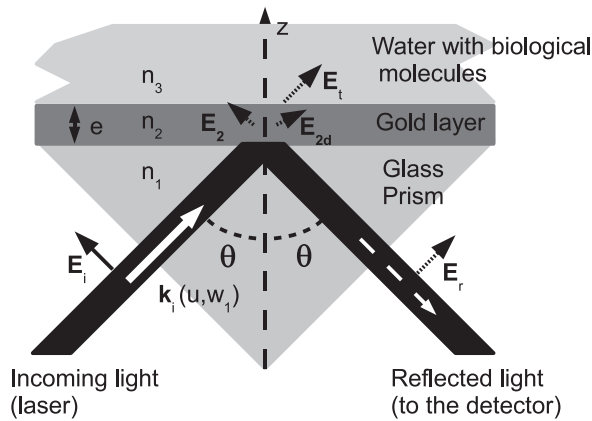


Fig. 1. Schematic of the SPR bio sensor, to be related to the Kretschmann configuration (Kretschmann, 1978).

The active part of the biosensor under consideration is the gold layer. The plasmon fingerprint corresponds to a strong decrease of R toward to 0 (Figs. 2). Therefore, the situation is slightly different from the classical electromagnetic one. In electromagnetics, the physical quantities of interest are the electromagnetic fields outside the material structures. The “input” is the incoming field and the “output” is the reflected and the transmitted fields. The (S) matrix relates the input to the output, for linear interaction of light with matter (Barchiesi, 1996; Li, 1996). On the contrary, in plasmonics, the system is the gold layer and the “output” of the system is the field inside the plate. Nevertheless, the transition between the two worlds is easy only if the property of resonance is correctly assessed. For this, the classical description of resonance by “getting something from nothing” is considered. Therefore, the field inside the gold layer must be related to the zero reflected field rather than the incoming field, through a (S') matrix. Assuming the reflected field expressed as proportional to the incoming field: $E_r = r.E_i$, the problem can be solved for plasmonics (Agarwal, 1973; Li, 1996; Raether, 1988; Simon et al., 1975). The field inside the metal film can be expressed as a sum of two fields E_2 and E_{2d} each of them associated to $\Re(w_2) > 0$ and $\Re(w_2) < 0$, w_2 being the normal to the slab components of the wave vector in gold (Fig. 1, (Born & Wolf, 1993; Simon et al., 1975)):

$$E_2 = \frac{t_{12}}{1 + r_{12}r_{23} \exp(2iw_2e)} E_i \tag{1}$$

$$E_{2d} = \frac{t_{12}r_{23} \exp(2iw_2e)}{1 + r_{12}r_{23} \exp(2iw_2e)} E_i, \tag{2}$$

with the interface coefficients of transmission and reflection (Fresnel's coefficients):

$$r_{i,i+1} = \frac{n_{i+1}^2 w_i - n_i^2 w_{i+1}}{n_{i+1}^2 w_i + n_i^2 w_{i+1}} \text{ and } t_{i,i+1} = \frac{2n_{i+1}^2 w_i}{n_{i+1}^2 w_i + n_i^2 w_{i+1}} \quad (3)$$

To describe the resonance and to express the (S') matrix, these fields should be expressed as functions of the reflected field E_r :

$$E_2 = \frac{t_{12}}{1 + r_{12}r_{23} \exp(2i w_2 e)} \frac{1 + r_{12}r_{23} \exp(2i w_2 e)}{r_{12} + r_{23} \exp(2i w_2 e)} E_r \quad (4)$$

$$E_{2d} = \frac{t_{12}r_{23} \exp(2i w_2 e)}{1 + r_{12}r_{23} \exp(2i w_2 e)} \frac{1 + r_{12}r_{23} \exp(2i w_2 e)}{r_{12} + r_{23} \exp(2i w_2 e)} E_r \quad (5)$$

The resonance corresponds to a pole of the scattering coefficients:

$$s'_1 = \frac{t_{12}}{r_{12} + r_{23} \exp(2i w_2 e)} \text{ and } s'_2 = \frac{t_{12}r_{23} \exp(2i w_2 e)}{r_{12} + r_{23} \exp(2i w_2 e)} \quad (6)$$

The pole occurs if the common term of these coefficients

$$s'_0 = \frac{t_{12}}{r_{12} + r_{23} \exp(2i w_2 e)} \quad (7)$$

$$= \frac{2n_2^2 w_1 (n_3^2 w_2 + n_2^2 w_3)}{(n_2^2 w_1 - n_1^2 w_2)(n_3^2 w_2 + n_2^2 w_3) + (n_3^2 w_2 - n_2^2 w_3)(n_2^2 w_1 + n_1^2 w_2) e^{2i w_2 e}} \quad (8)$$

is infinite, therefore, if the transcendent denominator vanishes. Obviously, the pole corresponds neither to the solution of $n_3^2 w_2 + n_2^2 w_3 = 0$ nor to that of $n_3^2 w_2 - n_2^2 w_3 = 0$.

Consequently, the solution of this last equation $n_1 \sin(\theta) = \pm \sqrt{n_2^2 n_3^2 / (n_2^2 + n_3^2)}$, cannot be likened to the condition of plasmon excitation in a gold plate. This last expression is actually the solution for the excitation of a plasmon in a semi-infinite metal medium.

Two arguments help to better understand this result. First, it is logical to find a dependence of the plasmon in a slab, as a function of the thickness of the layer e . Then, it is necessary to find consistence between the cancelation of R and the concept of resonance.

The basic model of SPR entails a single layer of gold (thickness e , optical index n_2) deposited on a glass substrate (optical index n_1) (Fig. 1). The above medium is water of optical index n_3 . The illumination is made by a p polarized plane wave, incoming on the gold layer under total internal reflection (TIR) configuration. θ is the angle between the illumination wave vector, and the normal to the layer vector. Figure 2(a) shows the computed reflected intensity $R = |r|^2$. The minimum of R depends on the thickness of the gold layer, therefore this parameter has to be optimized, to increase the efficiency of the biosensor in terms of contrast in R . The figure 2(b) shows the effect of a slight change in the optical index of the medium of detection n_3 : the position of the minimum is shifted toward larger angles. Therefore, to detect a change in the optical index n_3 of the above medium, the measurement of the shift of θ , corresponding to $R \approx 0$ is achieved (Bonod et al., 2003; Lecaruyer et al., 2006).

This setup is also called Kretschmann configuration (Kretschmann, 1978) and is an object of study for undergraduates, as r and t can be easily calculated (Simon et al., 1975). The reflection coefficient r has been used in Eq. 8 and can be written as:

$$r = r_{13}(e, \theta) = \frac{n_d}{d_d} = \frac{r_{12} + r_{23} e^{2i w_2 e}}{1 + r_{12} r_{23} e^{2i w_2 e}} \quad (9)$$

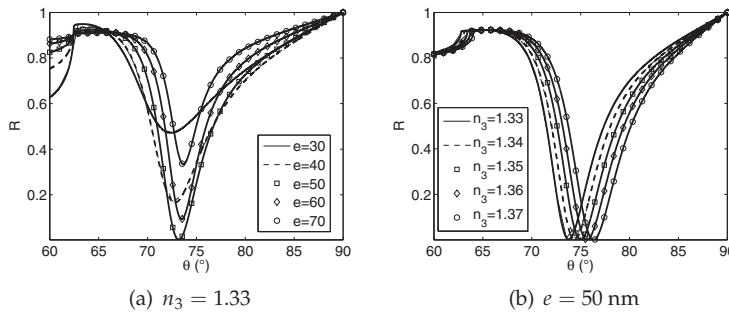


Fig. 2. Computation of the reflected field intensity $R = |r|^2$. The computation uses $n_1 = 1.5$, $n_2(\lambda_0 = 670 \text{ nm}) = 0.137 + 3.797i$.

The vertical components of the wave vectors in each medium i can be expressed as a function of the illumination angle θ : $w_i = \frac{2\pi}{\lambda_0} \sqrt{n_i^2 - n_1^2 \sin^2(\theta)}$, where n_i is the optical index (and is a complex number for metal). This expression is not relevant for numerical study as the denominators of each $r_{i,i+1}$ can cancel. Instead, reducing to a common denominator and simplifying the fraction is necessary before numerical optimization:

$$r = \frac{n}{d} = \frac{(n_2^2 w_1 - n_1^2 w_2)(n_3^2 w_2 + n_2^2 w_3) + (n_3^2 w_2 - n_2^2 w_3)(n_2^2 w_1 + n_1^2 w_2) e^{2\tau w_2 e}}{(n_2^2 w_1 + n_1^2 w_2)(n_3^2 w_2 + n_2^2 w_3) + (n_3^2 w_2 - n_2^2 w_3)(n_2^2 w_1 - n_1^2 w_2) e^{2\tau w_2 e}} \quad (10)$$

n is exactly the same as the denominator of s'_0 (Eq. 8) which cancels at the plasmon resonance. Figure 3(a) illustrates the influence of the reduction to the same denominator of r . Obviously, both formula (Eqs. 9 and 10) give the same square modulus: $R_d = |n_d/d_d|^2$ is superimposed with $R = |n/d|^2$. Nevertheless, wrong conclusions could be drawn from the visual inspection of $|d_p|$ and $|n_p|$. For instance, the plasmon resonance could be interpreted through the increase of $|d_p|$ and the decrease of $|n_p|$ and therefore by an apparent resonance behavior. These variations, in the vicinity of the plasmon angle, seems to be produced by the Fresnel's coefficient r_{23} , but the angle for plasmon resonance differs slightly from that corresponding to the maximum of $|r_{23}|$. $|n|$ and $|d|$ have very different bearing from $|n_d|$ and $|d_d|$: $|n|$ vanishes instead of $|d|$. The first inconsistency or deficiency of the classical $r = n_d/n_p$ model is evident in Fig. 3(a): at the plasmon resonance, the numerator $|n_d|$ is close to zero and the denominator is far from zero or infinity. Nevertheless, Figs. 3(a) and 3(b), based on the $r = n/d$ model, shows clearly that the R shape is mainly related to the cancelation of the numerator n . T is also plotted: it is the transmitted intensity of light and corresponds to evanescent wave ($n_3 < n_1$ and $\sin(\theta) > n_3/n_1$) and therefore is null. Therefore, even if the field amplitude differs from zero, $T = 0$. The increase of the square modulus of the fields in the gold layer is not governed by the r_{23} maximum but on field which is reflected by the Gold/Water interface (E_{2d} in Fig. 1). This latter takes into account the thickness of gold instead of r_{23} . The vertical lines in Fig. 3(b) shows the angular position of the maximum of $|r_{23}|^2$ and of the minimum of R . This last one is located between the positions of the maximum of $|E_{2d}|$ and of the local minimum of $|E_2|$. The plasmon launch can be explained by the coupling between these two fields (rather than the reflection coefficients of each interface).

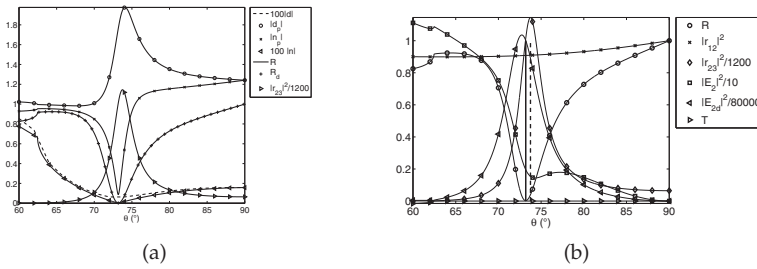


Fig. 3. (a) Reflected intensity $R = |r/n|^2$, and $|n_d/d_d|^2$ (Eqs. 9,10) and numerators and denominators: $|n|$, $|d|$, $|n_p|$ and $|d_p|$. (b) Plot of the amplitude of fields inside the gold layer $|E_2|$ and $|E_{2d}|$ and of the reflection coefficient on each interface (Glass/Gold: r_{12} and Gold/Water: r_{23} . All plot are functions of the angle of incidence θ , and are computed for $n_1 = 1.5$, $n_2(\lambda_0 = 670 \text{ nm}) = 0.137 + 3.797i$, $n_3 = 1.33$, $e = 50 \text{ nm}$.

Therefore, the accurate solution of plasmon launch corresponds to $n = 0$ ie:

$$n = 0 = \underbrace{(n_2^2 w_1 - n_1^2 w_2)(n_3^2 w_2 + n_2^2 w_3)}_{T_1} + \underbrace{(n_3^2 w_2 - n_2^2 w_3)(n_2^2 w_1 + n_1^2 w_2)}_{T_2} e^{2i w_2 e} \quad (11)$$

rather than:

$$n_3^2 w_2 - n_2^2 w_3 = 0 \Leftrightarrow \sin(\theta_{23}) = \pm \sqrt{\frac{1}{n_1^2} \frac{n_3^2 n_2^2}{n_3^2 + n_2^2}} \quad (12)$$

which is often considered (Agarwal, 1973; Raether, 1988). Nevertheless, this solution is a complex number, the optical index n_2 of gold being complex too. Therefore, practically, the resonance cannot be exactly reached, θ being real (Barchiesi, Kremer, Mai & Grosques, 2008; Maystre & Nevière, 1977; Maystre & Nieto-Vesperinas, 1992; Neff et al., 2006). This solution cancels the second term (T_2) of the sum in Eq. 11 and reduces the value of the first one (T_1) but is clearly not the optimum (figure 3(b)).

The discussion is now made easier. The plasmon launch requires p polarisation of the illumination and $n_3/n_1 < \sin(\theta)$ (configuration which differs from that considered by Agarwal for polaritons where $n_1 = n_3$ (Agarwal, 1973)).

- The plasmon resonance is measured by the strong attenuation of $R = |r|^2$ for a specific angle of incidence, close to that cancels the real part of the numerator of r .
- The real part of d vanishes for an angle of incidence far from the angle of plasmon resonance, but its modulus is never null. Indeed, the denominator of R is not vanishing.
- The angle of incidence of the minimum of R corresponds to the value which cancel the modulus of the numerator of r . The modulus of d slightly influence the result (Fig. 3(b)).
- near the resonance, $|r_{23}|$ is drastically increased. Nevertheless, the maximum of $|r_{23}|^2$ is not localized to that of plasmon resonance. Therefore, the classical approximation based on this reflection coefficient is not relevant and cannot be used for optimization. Moreover, this approximation lies in the conclusions we could draw too rapidly from a model assuming infinite thickness of metal. Indeed, the finite thickness of gold, enables the "coupling" of the surface plasmons.

For the SPR model, let us consider both interfaces Glass/Gold and Gold/Water for the SPR: $n_1 = 1.5, n_3 = 1.33$. Figure 4(a) shows the dispersion curve, deduced from the canceling of R for a gold layer of thickness 50 nm. The bottom of the black well in the map is the location of the plasmon, which abscissa are the angle of incidence θ and ordinates are the wavelength. At first glance, the plasmon can be launched for each wavelength and under small variations of θ . Therefore, the influence of the optical index n_2 of gold seems to be weak. *This fact explains why the bulk values of the gold optical index can be used and gives results close to the experiments, even if it is well known that this parameters depends strongly on the mode of gold deposition.* The white continuous curve delineate the bottom of the well. The cross are the values of $\theta_{r_{23}}$ for

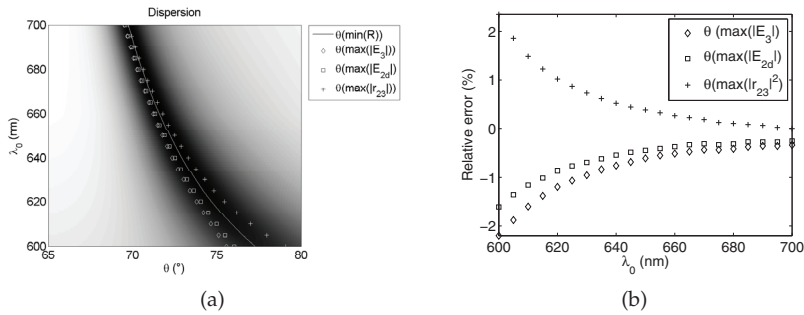


Fig. 4. (a) dispersion curve $R(\theta, \lambda_0)$. The line shows the minimum of the well, the crosses indicate the positions of $r_{23}(\theta, \lambda_0) = 0$, the diamonds those of $\theta(\max(|E_3|))$. The squares correspond to the location of the maximum for the down going field in gold (E_{2d}): this field can be seen as reflected by the Gold/Water interface but takes into account the thickness of the gold layer. (b) relative error between the above mentioned angles, and the angle corresponding to the minimum of R .

the maximum of the Fresnel's coefficient of the non coupled Gold/Water interface (n_i is the optical index n_2 of gold and $n_{i+1} = 1.33, n_1 = 1.55$ in Eqs. 3). The diamonds are the angle θ_3 for which $T = |t|^2$ is maximum, and the square are those θ_{2d} , for the maximum of the field reflected by the Gold/Water interface in the gold layer (taking into account the "coupling"). Figure 4(b) shows the relative difference between the above mentioned angles, and $\theta(\min(R))$, in %. Some conclusions can be drawn now:

- The relative error is not negligible for optimization but if only trends are awaited, all these angles can be used. $\theta_{r_{23}}$ is greater than the plasmon angle, while θ_{2d} and θ_3 are better approximation.
- The approximations are better if λ_0 raises.
- The better approximation is always θ_{2d} . One may conclude that the plasmon resonance is mainly governed by the field reflected by the Gold/Water interface. This explains why the SPR biosensor are sensitive to any change of the optical index of the above medium (here water). Nevertheless, the thickness of gold is a critical parameter and therefore any attempt to optimize the SPR by using $|r_{23}|$ would fail.

The figure 5 illustrates the possible cancelation of R (dark zones), as a function of the real part and the imaginary part of n_2^2 , the permittivity of the slab with virtual metallic optical index. For this, the thickness, the angle of incidence and the wavelength are fixed to $e = 50$ nm,

$\lambda_0 = 670 \text{ nm}$ and $\theta = 73^\circ$ (see Fig. 3(b)) to guarantee the possibility of plasmon launching. Despite all, r can be near zero for positive real part of the permittivity (n_2^2). The region of positive $\Re(n_2^2)$ define Brewster angle.

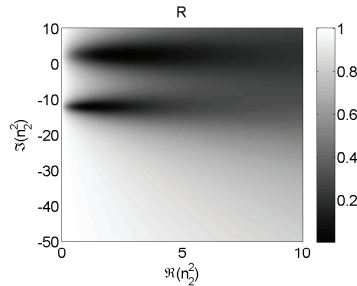


Fig. 5. R as a function of the permittivity of the layer virtual metallic material n_2^2 for $e = 50 \text{ nm}$, $\lambda_0 = 670 \text{ nm}$, $\theta = 73.2^\circ$, $n_1 = 1.5$, $n_3 = 1.33$ (Eq. 10).

The model of plasmon resonance is now well established. Nevertheless, the biosensor system is based on the detection of the angular shift of the minimum of R when n_3 varies. Therefore, the sensitivity of the biosensor must be investigated to determine if the simple minimization of R is sufficient.

2.2 The sensitivity of the SPR biosensor

The sensitivity of the SPR biosensor is related to the mode of detection. Basically, the quality of the plasmon resonance depends on the above mentioned parameters: the thickness of gold e , the wavelength λ_0 (and therefore the optical index of gold n_2) and the angle of incidence θ . But practically, a model of sensor must take into account the mode of detection of the angular shift of the plasmon resonance, under slight variations of the above optical index n_3 (Fig. 1). The detection of the angular shift is either monitored on the minimum of $R(\theta) = |r_{23}(\theta)|^2$ ($S_1 = \Delta\theta(\min(R))$), or on the maximum of slope $\max(|dR/d\theta|)$ of the same curve ($S_2 = \Delta\theta(\max(|dR/d\theta|))$). Figure 6 shows an illustration of these two modes as a function of the thickness e of the gold layer, with $n_3 = 1.330$, $\delta n_3 = 0.001$, $n_2(\lambda_0 = 670 \text{ nm}) = 0.137 + 3.797i$, $n_1 = 1.5$:

$$S_2 = \Delta\theta \left(\max \left(\left| \frac{dR}{d\theta} \right| \right) \right) = \theta \left(\max \left(\left| \frac{dR}{d\theta} (n_3 + \delta n_3) \right| \right) \right) - \theta \left(\max \left(\left| \frac{dR}{d\theta} (n_3) \right| \right) \right) \quad (13)$$

The maximum of the visibility of the recorded signal is $V = (\max(R) - \min(R)) / (\max(R) + \min(R))$. Near the plasmon resonance $\min(R) \approx 0$, but V decreases as a function of the detuning. Therefore V can be related directly to the quality of the plasmon resonance: Figs. 6(b) and 2 show that the maximum of visibility is reached when the plasmon occurs ($e \approx 52 \text{ nm}$ for $\lambda_0 = 670 \text{ nm}$). Moreover, even if maximizing the product $V \cdot S_2$ could be the natural target of optimization, the slight variations of the sensitivity curves can lead us to work directly on R . From here, we will try to find the best conditions of plasmon excitation *i.e.* R close to zero. Moreover, in both modes of detection, the sensitivity of the biosensor is governed by the shift of the peak and therefore exhibit the same behavior (Fig. 6(b)). Both sensitivities are increasing functions of the thickness. Therefore, the best conditions of detection are supposed to correspond to parameters closest to those of the ‘best’ plasmon

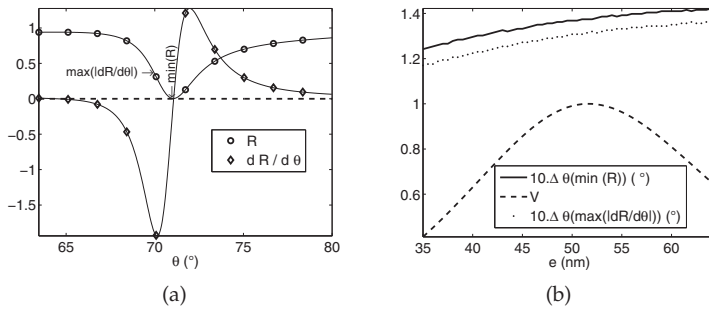


Fig. 6. (a) R and $dR/d\theta$ illustrating the two modes of detection as a function of θ . (b) Sensitivity of the biosensor as a function of the thickness of gold e , if the index of the medium of detection increases from $\delta n_3 = 0.01$. The sensitivities correspond to the angular shift of the plasmon resonance and to the shift of the maximum of the angular derivate of R . The visibility is $V = (\max(R) - \min(R)) / (\max(R) + \min(R))$. The parameters are $n_3 = 1.33$, $\lambda_0 = 670$ nm, $n_2 = 0.137 + 3.797i$, $n_1 = 1.5$.

resonance, where sensitivity is high enough as well as visibility, *ie* when the pole is close to the real axis.

Consequently, in the following, the goal of optimization will be the minimization of R , which is directly related to the quality of the plasmon resonance.

2.3 The optimization of the gold layer thickness

We have found the conditions of plasmon launch (Eq. 11). The optimization target of the plasmon resonance is therefore the smallest value of $R = |r|^2$. Practically, to launch an efficient plasmon for the SPR biosensor, the parameters to be optimized are the angle of incidence θ , the thickness of gold e , and the incoming wavelength λ_0 , the optical index of gold depending on the wavelength $n_2(\lambda_0)$. In principle, the wavelength can be imposed by the technical choice of the source of illumination and therefore, only two parameters remain free. The problem consists in finding the solutions of $|n| = 0$ (Eq 10). Even if this equation appears to be transcendent, the thickness of gold can be extracted:

$$e = -\frac{i}{2w_2} \log \left(-\frac{r_{12}}{r_{23}} \right) = -\frac{i}{2w_2} \log \left(-\frac{(n_2^2 w_1 - n_1^2 w_2)(n_3^2 w_2 + n_2^2 w_3)}{(n_3^2 w_2 - n_2^2 w_3)(n_2^2 w_1 + n_1^2 w_2)} \right) \quad (14)$$

If $n_2 = n_3$, this expression reduces to that of Eq. (2.28) in Ref. (Agarwal, 1973). Particular attention should be paid to the definition of the logarithm of complex number. It is not surprising that the mathematical solution for this thickness is a complex number. Therefore, the physical thickness e being real, the Poincaré’s plot of e in the complex plane, is an obvious tool for deterministic optimization (Barchiesi, Kremer, Mai & Grosgees, 2008). Both optimizations in Figs. 7 face a different methodology: Figure 7(a) consists in finding jointly the best values for e and θ , by minimizing R for each wavelength. Figure 7(b) is a Poincaré’s plot (Barchiesi, Kremer, Mai & Grosgees, 2008), in the phase plane of e , considering its complex value. These plots can help to choose the best set of parameters: thickness e , wavelength λ_0 , and the angle θ . The best thickness is closest to the real axis (the imaginary part of e is not physical). For example, a good set of parameters is $e = 52$ nm, $\lambda_0 = 750$ nm and $\theta = 68.2^\circ$.

This type of plot gives also information on the sensitivity of the model to the real part of e . For instance, the shelf, close to the maximum of the $\theta = 68.2^\circ$ curve, near $\lambda_0 = 670$ nm, corresponds to a zone of low sensitivity of the biosensor to the imaginary part of the thickness of gold, and therefore, a zone of stability. The same curve, near $\lambda_0 = 750$ nm, exhibits an infinite derivative, and therefore much less sensitivity to the thickness e .

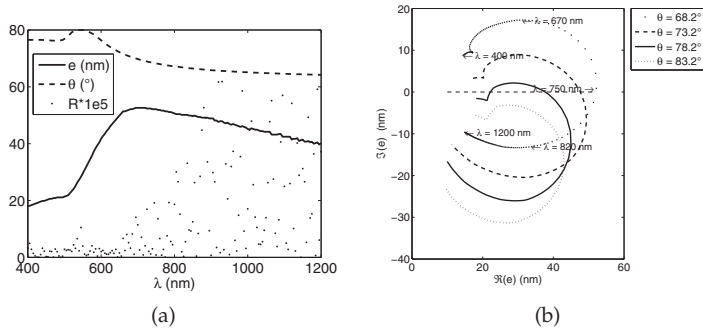


Fig. 7. Optimisation of angle θ and gold thickness e , the minimum of R is also plotted. Poincaré's plot of the best thickness e (Eq. 14), for various angles of incidence, as a function of the wavelength $\lambda_0 \in [400; 1200]$ nm.

It appears that even if the sensitivity of the SPR biosensor to the various parameters is a complex problem, it could be described by the model. The purpose of the next subsection is to evaluate the sensitivity of the model to the various parameters, through a comprehensive statistical method, where all parameters are considered simultaneously. This approach could help to evaluate the specifications for the design of biosensors.

2.4 Sensitivity of the model

The sensitivity of the model can help to evaluate what are the critical parameters in the process of fabrication of the biosensor. A Monte-Carlo method is one of the well known tools for the study of model's sensitivity. This method is based on the random generation of the endogenous parameters and on the statistical analysis of the output of the model. In the present case, a tolerance on $R \in [0, 10^{-3}]$ is fixed as well as physically acceptable interval for parameters (the input intervals in Tab. 1). To improve the efficiency of the Monte-Carlo method, an adaptation of the boundaries is proposed. A new random generation of N families \mathbf{p} of random parameters is repeated at each step of a loop, until the number of families \mathbf{p}_s making sure that $R(\mathbf{p}_s) \in [0, 10^{-3}]$ is greater than N . The boundaries of the space of search for each parameter are updated at each iteration, using the successful results of the previous loop. This adaptive boundary Monte-Carlo method enables to increase the number of "good" parameters \mathbf{p}_s , at each step, and therefore increases the convergence speed. For example, $N = 60.000$ requires less than 100 iterations in the loop. In the case of non adaptive Monte-Carlo method, the number of iterations is mostly greater than 1000. The pseudo-code of the adaptive Monte-Carlo algorithm is given (Algorithm 1).

The figure 8 shows the results that are summarized in the last column of Tab. 1 and the histograms for each parameters. The best value of the above realization of the Monte-Carlo software is also obtained: $R = 6.348 \times 10^{-5}$ for $e = 52.1$ nm, $\lambda_0 = 688$ nm, $\theta = 70.5^\circ$ and $n_3 = 1.331$. The histograms reveals a "mode" in the [600; 700] nm zone, which corresponds to

Require: α (threshold of tolerance on R), N (the number of random parameters set at each iteration). The initial boundaries of the hypercube D of acceptable parameters are set: $B_{min} = \{\min(e), \min(\lambda_0), \min(\theta), \min(n_3)\}$ and $B_{max} = \{\max(e), \max(\lambda_0), \max(\theta), \max(n_3)\}$.

- 1: [Initial random parameters set \mathbf{p} generated from uniform distribution in D : $U(D)$]
- 2: $\{\mathbf{y}\} \leftarrow R(\{\mathbf{p}\})$
- 3: [Selection of the $\{p\}$ that verify $\{\mathbf{y}\} < \alpha$]
 $\{\mathbf{p}_s\} \leftarrow \{\mathbf{p} \setminus \{\mathbf{y}\} < \alpha\}$
- 4: **while** [The sample size of \mathbf{p}_s is lower than N] **do**
- 5: $B_{min} \leftarrow \min(\mathbf{p}_s), B_{max} \leftarrow \max(\mathbf{p}_s)$
- 6: [Random generation of parameters $\{\mathbf{p}\}$ (uniform distribution in $[B_{min}, B_{max}]$: $U([B_{min}, B_{max}]))$]
- 7: $\{\mathbf{y}\} \leftarrow R(\{\mathbf{p}\})$
- 8: [Selection among the $\{p\}$ which verify $\{y\} < \alpha$]
 $\{\mathbf{p}_s^i\} \leftarrow \{\mathbf{p} \setminus \mathbf{y} < \alpha\}$
- 9: $\{\mathbf{p}_s\} \leftarrow \{\mathbf{p}_s\} \cup \{\mathbf{p}_s^i\}$
- 10: **end while**
- 11: $\min(\{\mathbf{p}_s\}), \max(\{\mathbf{p}_s\}) \dots$

Algorithm 1. Pseudo-code of the adaptive Monte-Carlo algorithm. The numerical model of the SPR is denoted R and is considered stable in D .

Parameter	Input interval	Output interval	mid-height size of the peak
$e(nm)$	[10; 80]	[43; 56]	[51.5; 52.5]
$\theta(^{\circ})$	[60; 80]	[68; 76]	[70.3; 70.8]
$\lambda_0(nm)$	[600; 700]	[600; 700]	[680; 695]
n_3	[1.33; 1.34]	[1.330; 1.339]	[1.330; 1.331]

Table 1. Parameters of the model, physically acceptable interval and tolerance revealed by the Monte-Carlo procedure. The output intervals correspond to $R < 10^{-3}$, and the statistical interval is defined by the mid-height size of the histogram of each parameter (Fig. 8).

$\lambda_0 = (682 \pm 10)$ nm, a thickness of gold $e = (52 \pm 1)$ nm, $\theta = (70.2 \pm 0.5)^{\circ}$ leading to a high sensitivity for n_3 (the peak is narrow). The sensitivity (or tolerance to variations) of parameters are obtained from the above results, and are indicated after the sign \pm . This study indicates that the tolerance on the thickness of gold must be better than 1 nm, that on the optical index of gold being deduced from the dispersion curve of gold in the interval [665; 700] nm *i.e.* $\Re(n_2^2) \in [-16.5; -14]$ and $\Im(n_2^2) \in [1.04; 1.06]$. This last result of this sensitivity study can be considered with confidence, knowing that optical characteristics of gold are very dependent modes of deposition. Thus, the real part of permittivity is a less critical parameter for the optimization of the biosensor, than its imaginary part. This result may explain the agreement between theory and experiment, generally obtained in plasmonics, even considering the bulk optical constants, and even the more or less accurate fits of these quantities (Drude of Drude-Lorentz for example) (Kolomenskii et al., 1997; Neff et al., 2006; Raether, 1988). Despite all, these models of dispersion cannot be used if accurate optimization is awaited, the data obtained from specific measurements would be more appropriate. Another output of the sensitivity study deserves to be highlighted: the shape (less than 0.001) of the peak in Fig. 8(d) gives preliminary informations on the sensitivity of the biosensor to slight changes in the optical index of the medium of detection.

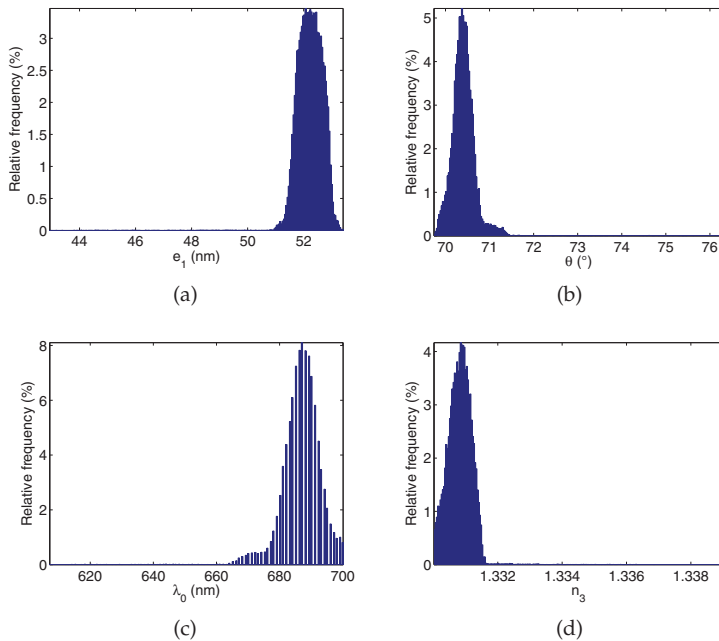


Fig. 8. Sensitivity study of the model of SPR. The involved parameters are the thickness of gold e , the angle of incidence θ , the wavelength of illumination λ_0 from which depends the optical index of gold n_2 , and the optical index of the medium of detection n_3 .

3. Some metaheuristic optimization methods for plasmonics

The model being established and characterized, the best values of the parameters are of interest. Models in plasmonics involve resonance and therefore the SPR is a good candidate to help to develop specific methods of optimization. Among them, two metaheuristics have been recently proposed (Barchiesi, 2009; Kessentini et al., 2011). The first one is selective and the second one is collaborative. The goal is to develop methods of optimization which could be efficient for problems in plasmonics with more degrees of freedom, especially the nanostructured biosensors. Nevertheless, to illustrate the optimization methods, we focus our study on the minimization of $R(e, \theta)$ to find the best set of parameters (e, θ) which is the most efficient to launch plasmon in the gold layer of the SPR biosensor. The wavelength of illumination is assumed to be fixed (so the index of gold), since it is imposed by choosing a laser source. In the following, we consider $\lambda_0 = 670$ nm. Of course this problem can always be solved by a systematic double loops study, but more general problems in plasmonics involve more than two parameters, and the goal is to develop a rapid method of optimization for this more general case.

The present problem being of dimension $N = 2$ (two parameters are searched: $\mathbf{p} = (\theta, e)$), a plot of R illustrates the topology of the function $R(e, \theta)$. Figure 9 exhibits the track of plasmon in the map of R , its location and shape. As expected, the best parameters for the plasmon launch, are located in a wells which shape depends on the wavelength.

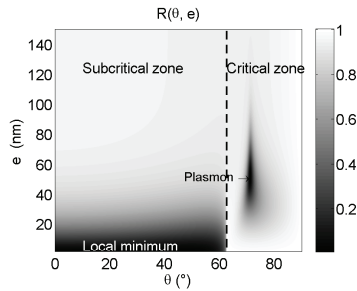


Fig. 9. Fitness function for the optimization: $R(\theta, e)$, for $n_1 = 1.5$, $n_2 = 0.1373 + 3.7975i$ ($\lambda_0 = 670$ nm), $n_3 = 1.33$.

In this case, the solution of the optimization can be easily determined. This problem is therefore a test for the following optimization methods.

3.1 Evolutionary method: a selective method

Among the numerous optimization schemes, the evolutionary methods are parts of the metaheuristics, based on the mimicry of nature, with the numerical mutation of the parameters considered as genes, and the selection of the bests for the breeding of the next generation (Schwefel, 1995). However, despite the apparent simplicity of the statistical method, its effectiveness depends on the addressed problem. Here, in plasmonics, the detection of sharp resonances through looking for a minimum of a complex function is under consideration. The balance between speed and diversity of research, particularly the ability to avoid local minima but to find the global optimum, must be studied carefully. In this section, we describe the classical evolutionary scheme (Schwefel, 1995) and one of its improvement (Barchiesi, 2009).

The target is the minimization of the fitness function $R(e, \theta)$ in a domain of acceptable parameters, n_3 being fixed (Fig. 1). This minimum corresponds to the best transfer of energy from the illumination to the gold layer.

The evolutionary scheme consists in four steps: initialization, recombination, mutation and selection. This process is repeated for several generations. A first population (parents) with μ parameters set (or elements) $\mathbf{p}_{m=1..\mu} = (\theta_m, e_m)$, is randomly generated. Then the parents breed to give birth to offspring (λ children): $\mathbf{p}'_{m=1..\lambda} = (\theta_i, e_i)$ (cross-over). The children mutation is used to increase the diversity of search. The selection of the μ best parameters enables to retain only the best performing in terms of fitness function. The selection is made through an elitist or non-elitist process, the first one involving also the parents in the choice of the best ones (the performance of the $\mu + \lambda$ elements is compared). A funny remark deserves to be made at this step: the elitist process is immoral because it will allow reproduction between children and parents to the next generation. The evolutionary algorithm requires strategy parameters s which enable to control the convergence of mutation (Schwefel, 1995). The pseudo-algorithm 2 presents the steps of computation. The classical evolutionary algorithm 2 (SEM) is generic, and the crossover and mutations are unattached on the quality of the elements. Therefore, depending on the mathematical properties of the N -dimensional function R , the convergence can slow down, especially if the solution is in a narrow wells. The classical recombination uses fixed weights (Donnel & Waagen, 1995) or uniformly distributed weights for each element (Yang et al., 1997).

Classical Evolutionary Method (SEM)

Require: D domain of the N acceptable parameters $e, \theta \dots$

Require: Fixed parameters of the model R .

Require: λ, μ, T (maximum of generations), SC stop criterion, ρ number of elements to be recombined, strategy parameters $\tau_1 \leftarrow (2.N)^{-1/2}, \tau_2 \leftarrow (2.\sqrt{N})^{-1/2}$
 $\sigma \leftarrow 1$

- 1: [Initial population, with normal distribution of probability G or uniform law U in D]
 $s_{m=1..μ} \leftarrow \sigma.D$
 $p_{m=1..μ} \leftarrow G(D)$ or $U(D)$
 $y_{m=1..μ} \leftarrow R(p_{m=1..μ})$
- 2: **while** $|y_1 - y_μ| / |y_1 + y_μ| > SC$ **do**
- 3: [Blind cross-over with random choice of integers n through $U(\{1, \dots, \mu\})$]
 $s'_{m=1..λ} \leftarrow \rho^{-1} \sum_{\rho} s_n$
 $p'_{m=1..λ} \leftarrow \rho^{-1} \sum_{\rho} p_n$
- 4: [Normal law mutation, G_i are normalized normal distribution of probability (Schwefel, 1995)]
 $s''_{m=1..λ} \leftarrow s'_{m=1..λ} \cdot \exp(\tau_1.G_2 + \tau_2.G_2)$
 $p''_{m=1..λ} \leftarrow p'_{m=1..λ} + G_3.s''_{m=1..λ}$
- 5: [Selection (sort operator $S()$) of the μ best elements for the initial population of the next step]
- 6: **if** [Non Elistist] **then**
- 7: $y_{m=1..λ} \leftarrow R(p''_j)$
 $p_{m=1..μ} \leftarrow S(\{p''_{m=1..λ}\})$
- 8: **else if** [Ellistist] **then**
- 9: $y_{m=1..μ+\lambda} \leftarrow R(\{p''_j, p_j\})$
 $p_{m=1..μ} \leftarrow S(\{p''_{m=1..λ}, p_{m=1..μ}\})$
- 10: **end if**
 $s_{m=1..μ} \leftarrow s''_{m=1..μ}$
- 11: **end while**

Adaptive Non Uniform Hyper Elistist Method (ANUHEM)

Require: D domain of the N acceptable parameters $e, \theta \dots$

Require: Fixed parameters of the model R .
Require: λ, μ, T (maximum of generations), SC stop criterion, ρ number of elements to be recombined.

- 1: [Initial population with U : multidimensional uniform law in D]
 $p_{m=1..μ} \leftarrow U(D)$
 $y_{m=1..μ} \leftarrow R(p_{m=1..μ})$
- 2: **while** $|y_1 - y_μ| / |y_1 + y_μ| > SC$ **do**
- 3: [Hyper-Elistist cross-over with random choice of integers n through $U(\{1, \dots, \mu\})$]
 $p'_{m=1..λ} \leftarrow \sum_{\rho} y_n^{-1} p_n / \sum_{\rho} y_n^{-1}$
- 4: [Adaptive Non-Uniform mutation using topology of solutions]
 $b \leftarrow std(p_{m=1..μ}) / std(y_{m=1..μ})$
 $\sigma \leftarrow 1 - U([0; 1])^{(1-g/T)^b}$
 $p''_{m=1..λ} \leftarrow U_b(D, \sigma) \{U_b(D, \sigma):$
 multidimensional non uniform law in D with constraints $p'' \in D\}$
 $y_{μ+1..μ+\lambda} \leftarrow R(p''_j)$
- 5: [Selection (S) of the μ best elements for the initial population of the next step]
- 6: **if** [Non Elistist] **then**
- 7: $p_{m=1..μ} \leftarrow S(\{p''_{m=1..λ}\})$,
- 8: **else if** [Ellistist] **then**
- 9: $p_{m=1..μ} \leftarrow S(\{p''_{m=1..λ}, p_{m=1..μ}\})$
- 10: **end if**
- 11: **end while**

Algorithm 2. Pseudo-codes of Evolutionary Methods. R is the fitness function.

An alternative method, keeping the information on the quality of parameters during the breeding step has been proposed (Barchiesi, 2009). This Hyper-Elistist scheme (ANUHEM) is based on the balance between the variety of search (which is necessary to prevent attraction to local minima of R) through the non uniform law, and the dominance of high quality elements. The hyper elitist breeding using weighted recombination (barycentric crossover), prevents the lost of a small number of solutions near the global minimum of R . Instead, the non-uniform mutation counterbalances this strong attraction, and enables to keep the variety of search in D . The corresponding pseudo-code is on the right of Algorithm 2, to facilitate the comparison.

The ANUHEM is partially inspired by the Cooperative-Competitive scheme applied to radial basis functions networks in Ref. (Whitehead & Choate, 1996). Five cases have to be distinguished, considering $\rho = 2$ to simplify the discussion:

- If the two recombined elements are close to a global minimum of R : the weighting facilitates the convergence towards this minimum.
- If the two recombined elements are close to two separate local minimums, the offspring is near the “best” of the two ones.
- If only one recombined elements is near the global minimum, the other one may be near a local minimum of R : the recombined element is attracted by the global minimum.
- If the two recombined elements are away from the global minimum: the effect of the weighting used in recombination is lessened. The whole search space is surveyed, like with the Schwefel’s recombination.
- If the two elements are close to a local minimum of R : the convergence of the algorithm to this minimum is prevented by mutation.

The mutation process in SEM uses the Gaussian distribution and the adaptation of its standard deviation, to produce offspring. Other algorithms use Cauchy or Lévy probability distributions (Lee & Yao, 2004; X. Yao & Lin, 1999). To avoid useless evaluations of R after the mutation process, which can generate offspring that are out of the domain of possible parameters, a uniform probability law is preferred. This choice is also governed by the strong local capacity escape of the uniform mutation operator (Gunter, 1997). To avoid the possible convergence toward a local minimum, the operator used in the ANUHEM is actually a “Non-Uniform” mutation proposed by Michalewicz (Michalewicz, 1992) and used for example in (Alfaro-Cid et al., 2005; Zhao et al., 2007). However, in this study, the operator has been somewhat modified as following, to deal with the detection of poles:

$$\mathbf{p}_n'' = \mathbf{p}_n' + [(U_n - \mathbf{p}_n') \cdot B(0.5, 2) - (\mathbf{p}_n' - L_n) \cdot (1 - B(0.5, 2))] \cdot (1 - U^{(1-g/T)^b}), \quad (15)$$

where U_n and L_n are the upper and lower bounds of the allowed parameters (domain D of physically acceptable values), $B(0.5, 2)$ is the Bernoulli’s distribution with probability $p = 0.5$ and evaluated for each parameter, U is the normalized uniform distribution (in $[0, 1]$), g the generation of the evolutionary loop, T is the maximal generation number (arbitrary fixed at the beginning of the evolutionary loop) and b is a system parameter determining the degree of non uniformity (Zhao et al., 2007). In Ref. (Zhao et al., 2007), an adaptive scheme was proposed. Three possible test parameters were tested to generate offspring from the same parent, and the best one was the survivor. In this study, such a parameter cannot be fixed, due to the inhomogeneity of the fitness function. The inhomogeneity of R is given by the ratio of the standard deviation of the initial population to the standard deviation of the fitness function:

$$b = \frac{\text{std}(\mathbf{p}_i)}{\text{std}(R(\mathbf{p}_i))}. \quad (16)$$

and the non uniform distribution is given by:

$$U_b = 1 - U^{(1-g/T)^b}. \quad (17)$$

b is related to the “slope” of the solutions, in other words, to the spreading (or dispersion) of the initial population with regards to their quality, and is therefore adapted for each generation. b can differ for each of the two parameters (e, θ) and therefore takes into account the “sensitivity” of R to the variations of both parameters. At the beginning of the evolutionary loop, b is close to $(U_n - L_n)$ and the mutation is very sensitive to the variations of the fitness function and therefore to the quality of parameters. When the evolutionary algorithm converges to the global optimum, the local slope of the wells decreases like b , and the mutation operator exploration is more efficient in the wells.

Finally, in both methods (SEM and ANUHEM), the elitist selection is made among the initial and mutated elements, at each step of the evolutionary loop. Therefore, this elitist selection uses the evaluation of the quality of the parents and of the offspring (method $(\lambda + \mu) - ES$). This hyper-elitist method requires the evaluation of the fitness function with any element p_n and p_n'' . Thus, these methods require time as the model used in the fitness function R must be evaluated $\mu + \lambda$ times per generation. The goal is therefore to decrease the required number of generations to reach convergence to one of the global minimums (and to detect the possible resonances).

The termination criterion is based on the convergence of the evolutionary method, the value of the global minimum being unknown in the general case. Therefore the stopping criterion is:

$$\left| \frac{R(e_\mu, \theta_\mu) - R(e_1, \theta_1)}{R(e_\mu, \theta_\mu) + R(e_1, \theta_1)} \right| < TC = 10^{-3} \quad (18)$$

When the termination criterion is reached, the evolutionary loop is stopped and a Nelder-Mead Method can be used to achieve the convergence toward the minimum of the wells of the function and to obtain the final set of parameters. Before evaluating the performances of both schemes on SPR, we introduce another method that is more collaborative than selective: the Particle Swarm Method.

3.2 Particle Swarm method: a collaborative method

The Particle Swarm Optimization (PSO) was first introduced by Kennedy and Eberhart in 1995 and imitates the swarm behaviour to search the globally best solution, which is considered as pollen for bees swarm (Kennedy & Eberhart, 1995). The swarm of parameters searches the best solution of a problem through collaboration. This metaheuristic method is based on the time dependent movement of parameters in the search space, toward the optimum. Actually, selection processes are not used in PSO, instead, reasonable displacements are chosen, based on the experience of parameters. The PSO (Kennedy & Eberhart, 1995) as well as Evolutionary Methods (Schwefel, 1995) are direct search, stochastic methods, used to find an optimal solution of a problem, described by a model, considered as a black box. So the model should be as stable as possible in the field of original research acceptable parameters. Divergences are not tolerable in the search intervals, under penalty of a failure of optimization. Contrariwise, discontinuities in the model are accepted, and test functions have been developed to check the optimization methods in that case. In plasmonics, as we noted above, one can always transform the model so that the goal becomes finding a minimum in a narrow well.

For all optimization methods, and especially metaheuristics, a universal scheme does not exist. Many improvements have been proposed, particularly to make them more effective for solving specific problems (Hu & Eberhart, 2002; Kennedy & Mendes, 2002; Liang et al., 2006; Mendes et al., 2004; Veenhuis, 2006). The main issues that have to be addressed are following:

- balancing between efficiency and rapidity: the decrease of the time of execution is critical, especially if the model requires huge computational time; but this conducts inevitably to increase the probability of attraction to any of the local optimum. The diversity of search is counterbalanced by the convergence time of the optimization;
- preventing the useless evaluations: in the evolutionary methods, the blind breeding of parameters can conduct to reduce the efficiency of method, as well as the outflow of domain for PSO.

The PSO is basically cooperative method where the set of parameters \mathbf{p} at step t (corresponding to generation g in evolutionary methods) is considered as a moving particle (or bee) in the N -dimensional space of search. The particles of a swarm communicate good positions to each other and adjust their own positions \mathbf{p} and velocities \mathbf{v} at each step t :

$$\mathbf{v}(t+1) = \omega\mathbf{v}(t) + r_1c_1(\mathbf{p}_b(t) - \mathbf{p}(t)) + r_2c_2(\mathbf{p}_b - \mathbf{p}(t)) \quad (19)$$

$$\mathbf{p}(t+1) = \mathbf{p}(t) + \mathbf{v}(t+1) \quad (20)$$

where r_1 and r_2 are random variables between 0 and 1, $\mathbf{p}_b(t)$ is the particle best position, \mathbf{p}_b is the global best, ω is the inertial weight and c_1 and c_2 are the acceleration coefficients. The parameters ω , c_1 and c_2 could be constant or time dependent (i.e. updated at each step). After computing the new velocity, the particle moves toward a new position following Eq. 20. The particle new velocity $\mathbf{v}(t+1)$ combines its previous value and the distances between the particle current position and its own best found position i.e. its own best experience $\mathbf{p}_b(t)$ and the swarm global best \mathbf{p}_b . The first term of Eq. 19 is an inertia term which prevents the only local search and therefore preserves diversity in the exploration of D . Nevertheless, the inertia weight, introduced by Shi and Eberhart (Shi & Eberhart, 1998), is linearly decreasing from 0.9 to 0.4, in classical PSO. The acceleration coefficients c_1 and c_2 are generally fixed to $c_1 = 0.738$ and $c_2 = 1.51$, values that have been determined as optimal for the resolution of simple problems (Clerc, 2009) but significant efforts have been worn for improving the choice of these exogenous parameters (Zhan et al., 2009), leading to an adaptive method, by the estimation of the search state at each step. Four search states have been identified: exploration, exploitation, convergence and jumping out (Zhan et al., 2009) and adapted strategies are used to update the inertia weight and the acceleration coefficients. Finally, to avoid local optima, an elitist learning of the convergence state will permit the jump out of the likely local optima. Nevertheless, some general rules have been established to choose the cognitive parameter c_1 and the social parameter c_2 : $c_1 + c_2 < 4$ with possible priority to cognition (Carlisle & Dozier, 2001).

In the present study, we use standard PSO as reference with $c_1 = c_2 = 2$, that seems to be the most efficient choice of exogenous parameters. And we also propose an adaptive method based on the same principle as in the ANUHEM method (Barchiesi, 2009): the ANUPSO (Adaptive Non Uniform Particle Swarm Method) (Kessentini & Barchiesi, 2010a; Kessentini et al., 2011). Actually, for the plasmonic problems, a compromise between diversity search and convergence speed-up to the global optimum must be found. Consequently, the proposed adaptive PSO algorithm, will exploit topological information gathered about fitness function $R(\mathbf{p})$ at each iteration. The initialization of variables and speed for each particle is carried following the scheme proposed by Clerc (Clerc, 2009):

$$\mathbf{v}(1) = 0.5(\max(D) - \min(D)) \text{ and } \mathbf{p}(1) = U(D) \quad (21)$$

Then, the adaptation of the exogenous parameters is ensured through the non-uniform law (Eq. 17), with $b(t)$ defined in Eq. 16 :

$$\omega(t) = \max(b(t)) \text{ and } c_1 = 2U_{b-1}, c_2 = 2U_{b-1} \quad (22)$$

The domain of variation of c_i is set to include the classical values used for PSO that are mentioned above, as well as the constraint $c_1 + c_2 < 4$. All the adaptive parameters are therefore monitored by the topology of the fitness function R . Actually, $b(t)$ can be seen as the slope of the solutions, i.e. the spreading/ dispersion of the population with regards to their quality. $b(t)$ can differ for each component of $\mathbf{p}(t)$ and therefore takes into account the sensitivity of R to the variations of all parameters of \mathbf{p} . The only exogenous parameter is T . $b(t)$ determines the degree of non-uniformity (Zhao, 2008): the diversity of parameters increases instead the average speed of the diversity decreases, when $b(t)$ increases.

The proposed adaptive PSO (ANUPSO) can be compared to the method proposed in (Zhan et al., 2009) where the authors outlined the necessity of updating the acceleration coefficients following the three phases of optimization that are expected during the PSO loop (exploration, exploitation or convergence phase). Through the value of $b(t)$:

- ω , the inertial coefficient, is close to one in the exploration phase, then decreasing, then increasing in the exploitation state. This preserves the diversity of solutions and prevents the convergence to a local minimum. Finally it decreases toward 0 in the convergence state (when many particles are close to those for the global minimum).
- c_i , the acceleration coefficients tends toward 0 when t reaches T (Zhao, 2008)). Therefore T controls convergence and remains the only non-adaptive parameter of the method.

The values of $b(t)$, for each parameter, governs the convergence speed-up as follows:

- In the exploration state, $b(t)$ is close to one as well as $c_1(t)$ and $c_2(t)$. The value of $b(t)$ gives equal weight to the different contributions of the velocity. If the speed of the particle is too high, the particle (obtained at the generation t) leaves the search space and is therefore replaced by a random particle, through a uniform law, as in the initialization step. This contributes to the diversity at this stage.
- In the exploitation state, $b(t)$ increases and also the convergence speed-up (Zhao, 2008)
- In the final state of convergence, $b(t)$ decreases again and the wells of the objective function R are more carefully exploited.

An illustration of the performances of the the four methods is following.

3.3 Numerical study of the selective and collaborative methods

The problem under investigation is the SPR, assuming only two optimized parameters, as considered above. The best values of the thickness e of the gold layer, and of θ , the angle of illumination are searched, the goal being the minimization of $R(\theta, e)$ (Figure 9). The model is used as a black box for each method of optimization, the optimization is repeated at least 10.000 times to compute the statistics of success (converging before T generations to a solution close to the optimum) and of the number of evaluations of the model R . Let us underline again, that such method of optimization is designed to deal with much more complex models, and $\dim(D) \gg 2$. Therefore, the optimization must avoid useless evaluations of a time consuming model. The table 2 shows the performances of SEM, ANUHEM, PSO and ANUPSO. The domain of search is $D = [1; 80] \text{ nm} \times [\arcsin(\sqrt{\epsilon_3/\epsilon_1}); \pi/2]$. This domain is wide enough to set default behavior of the methods. The evolutionary method will give trivial

solutions, out of the initial domain, corresponding to a null thickness of gold for example. The classical PSO freezes the too fast particles that would get out the domain D . Therefore, these particles are lost for the iteration of the search process. Some solutions have been proposed to overcome this problem, but are out of the scope of this study (Kessentini & Barchiesi, 2010b). Moreover, keeping in mind the objective of limiting the number of evaluations, we limit the number of generations (or iterations) to $T = 400$. This is very constraining with regards to the classical way of bench, for which this exogenous parameter is not limited. Of course, the success rate approaches 100% for all methods, if $T > 1000$ in this case. We also fix $\mu = 5$, $\lambda = 25$ and therefore the number of particles in swarm to 30. This small number of parameters is also an encumbrance for the optimization methods. This simple test, even if only two parameters have to be optimized, pushes the methods in trenches (Tab. 2).

	SEM	ANUHEM	ANUPSO	PSO
success (%)	90%	100%	100%	100%
mean number of evaluations	6800	172	167	962

Table 2. Elitist SEM and ANUHEM, with $\lambda = 25$ and $\mu = 5$. ANUPSO and PSO, success rate and mean number of evaluations in case of success. To be considered as successful, the number of generation must be less than $T = 400$ to be considered as successful. The PSO uses $N = 30$, $c_1 = 2$, $c_2 = 2$ and ω linearly decreasing from 0.9 to 0.4. The best parameters are $e = 51$ nm and $\theta = 71^\circ$.

Table 2 shows that the classical methods are of course non universal and especially not convenient for plasmonics. Both improvements, using non-uniform law seem to be efficient. The best methods, under the above mentioned strong constraints are clearly the ANUPSO and the ANUHEM. Let us note that the selection scheme is elitist in this study. If not, the success rate would be worse and the number of evaluations would be increased. This illustration shows that an ideal and versatile method of optimization does not exist. Instead, some improvements have to be made to hope to reach a sufficient level of reliability. Despite all, the systematic study of double loop would require at least ten times evaluations to get the same accuracy on the optimized values.

Some of these heuristic methods have been used successfully, to optimize metal nanoparticles for the cancer therapy and imaging (Grosjes, Barchiesi, Toury & Gréhan, 2008) and multilayered SPR (Barchiesi, Macías, Belmar-Letellier, Van Labeke, Lamy de la Chapelle, Toury, Kremer, Moreau & Grosjes, 2008) and we hope to succeed in appliance to the more complex nanonatennas (www.nanonatenna.eu).

4. Conclusion

The numerical optimization of biosensors is necessary to spare time and money. In the case of plasmonics biosensors, modeling accurately the sensor is still a challenge. However, the numerical optimization requires a stable and accurate model, to be used as a black box for optimization. Even, if the model seems simple: the above model of SPR has been used for illustration, we have shown that the plasmon resonance is a tedious phenomenon, and a deep understanding of the model is necessary before optimization. On the other hand, the optimization methods themselves have to be carefully improved and tested before application to plasmonics. This still remains an open domain for physicists, biologists and theoreticians, but hopefully, solutions seem now begin to emerge.

5. References

- Agarwal, G. S. (1973). New method in the theory of surface polaritons, *Phys. Rev. B* 8(10): 4768–4779.
- Alfaro-Cid, E., McGookin, E. W. & Murray-Smith, D. (2005). A novel non-uniform mutation operator and its application to the problem of optimising controller parameters, *IEEE Congress on Evolutionary Computation* 2: 1555–1562.
- Barchiesi, D. (1996). A 3-D multilayer model of scattering by nanostructures. application to the optimisation of thin coated Nano-Sources, *Optics Commun.* 126: 7–13.
- Barchiesi, D. (2009). Adaptive non-uniform, hyper-elliptic evolutionary method for the optimization of plasmonic biosensors, *International Conference on Computers & Industrial Engineering* pp. 542–547.
- Barchiesi, D., Guizal, B. & Grosjes, T. (2006). Accuracy of local field enhancement models: Toward predictive models?, *Appl. Phys. B* 84: 55–60.
- Barchiesi, D., Kremer, E., Mai, V. & Grosjes, T. (2008). A Poincaré's approach for plasmonics: The plasmon localization, *J. Microscopy* 229: 525–532.
- Barchiesi, D., Macías, D., Belmar-Letellier, L., Van Labeke, D., Lamy de la Chapelle, M., Toury, T., Kremer, E., Moreau, L. & Grosjes, T. (2008). Plasmonics: Influence of the intermediate (or stick) layer on the efficiency of sensors, *Appl. Phys. B* 93: 177–181.
- Billot, L., de la Chapelle, M., Grimault, A. S., Vial, A., Barchiesi, D., Bijeon, J.-L., Adam, P.-M. & Royer, P. (2006). Surface enhanced raman scattering on gold nanowire arrays: Evidence of strong multipolar surface plasmon resonance enhancement, *Chem. Phys. Lett.* 422(4-6): 303–307.
- Bonod, N., Enoch, S., Li, L., Popov, E. & Nevère, M. (2003). Resonant optical transmission through thin metallic films with and without holes, *Opt. Express* 11(5): 482–490.
- Born, M. & Wolf, E. (1993). *Principle of Optics*, Pergamon Press, Oxford.
- Carlisle, C. & Dozier, G. (2001). An off-the-shelf PSO, *Proc. Particle Swarm Optimization Workshop*, pp. 1–6.
- Clerc, M. (2009). A method to improve standard PSO, *Technical Report DRAFT MC2009-03-13*, France Telecom R&D.
- Donnel, J. M. & Waagen, D. (1995). An empirical study of recombination in evolutionary search, *Proc. Of the Fourth Annual Conference on Evolutionary Programming*, pp. 465–478.
- Ekgasit, S., Thammacharoen, C., Yu, F. & Knoll, W. (2005). Influence of the metal film thickness on the sensitivity of surface plasmon resonance biosensors, *Appl. Spectroscopy* 59: 661–667.
- Grosjes, T., Barchiesi, D., Toury, T. & Gréhan, G. (2008). Design of nanostructures for imaging and biomedical applications by plasmonic optimization, *Opt. Lett.* 33(23): 2812–2814.
- Grosjes, T., Borouchaki, H. & Barchiesi, D. (2007). Improved scheme for accurate computation of high electric near-field gradients, *Opt. Express* 15(3): 1307–1321.
- Grosjes, T., Borouchaki, H. & Barchiesi, D. (2008). New adaptive mesh development for accurate near-field enhancement computation, *J. Microscopy* 229(2): 293–301.
- Grosjes, T., Borouchaki, H. & Barchiesi, D. (2010). Three dimensional adaptive meshing scheme applied to the control of the spatial representation of complex field pattern in electromagnetics, *Appl. Phys. B* 101: 883–889.
- Grosjes, T., Vial, A. & Barchiesi, D. (2005). Models of near-field spectroscopic studies: Comparison between finite-element and finite-difference methods, *Opt. Express* 13: 8483–8497.

- Gunter, R. (1997). Local convergence rates of simple evolutionary algorithms with Cauchy mutations, *IEEE Trans. Evol. Comput.* 4: 249–258.
- Hoaa, X., Kirk, A. & Tabrizian, M. (2007). Towards integrated and sensitive surface plasmon resonance biosensors: A review of recent progress, *Biosensors and Bioelectronics* 23: 151–160.
- Hu, X. & Eberhart, R. (2002). Multiobjective optimization using dynamic neighborhood particle swarm optimization, *Proc. IEEE Congress Evolutionary Computation*, IEEE, Honolulu, HI, pp. 1677–1681.
- Kennedy, J. & Eberhart, R. (1995). Particle swarm optimization, *IEEE International Conference on Neural Networks*, IEEE, Path, Australia, pp. 1942–1948.
- Kennedy, J. & Mendes, R. (2002). Population structure and particle swarm performance, *IEEE Congress Evolutionary Computation*, IEEE, Honolulu, HI, pp. 1671–1676.
- Kessentini, S. & Barchiesi, D. (2010a). A new strategy to improve particle swarm optimization exploration ability, *Intelligent Systems (GCIS), 2010 Second WRI Global Congress on*, Vol. 1, IEEE, pp. 27 – 30.
- Kessentini, S. & Barchiesi, D. (2010b). A new strategy to improve particle swarm optimization exploration ability, *2010 Seconde WRI Global Congress on Intelligent Systems*, IEEE, Wuhan, China, pp. 27–30.
- Kessentini, S., Barchiesi, D., Grosge, T., Giraud-Moreau, L. & de la Chapelle, M. L. (2011). Adaptive non-uniform particle swarm application to plasmonic design, *International Journal of Applied Metaheuristic Computing (IJAMC)* 2(1): 18–28.
- Kolomenskii, A., Gershon, P. & Schuessler, H. (1997). Sensitivity and detection limit of concentration and absorption measurements by laser-induced surface-plasmon resonance, *Appl. Opt.* 36: 6539–6547.
- Kretschman, E. & Raether, H. (1968). Radiative decay of nonradiative surface plasmons excited by light, *Z. Naturforsch. A* 23: 2135–2136.
- Kretschmann, E. (1978). The ATR method with focused light - application to guided waves on a grating, *Optics Commun.* 23(1): 41–44.
- Lecaruyer, P., Maillart, E., Canva, M. & Rolland, J. (2006). Generalization of the rouard method to an absorbing thin-film stack and application to surface plasmon resonance, *Appl. Opt.* 45: 8419–8423.
- Lee, C. Y. & Yao, X. (2004). Evolutionary programming using mutations based on the lévy probability distribution, *IEEE Trans. Evol. Comput.* 8: 1–13.
- Li, L. (1994). Multilayer-coated diffraction gratings: Differential method of chandezon et al. revisited, *J. Opt. Soc. Am. A* 11: 2816–2828.
- Li, L. (1996). Formulation and comparison of two recursive matrix algorithms for modeling layered diffraction gratings, *J. Opt. Soc. Am. A* 13(5): 1024–1035.
- Liang, J. J., Qin, A., Suganthan, P. N. & S.Baskar (2006). Comprehensive learning particle swarm optimizer for global optimization of multimodal functions, *IEEE Transactions in Evolutionary Computing* 10(3): 281–295.
- Macías, D., Vial, A. & Barchiesi, D. (2004). Application of evolution strategies for the solution of an inverse problem in Near-Field Optics, *J. Opt. Soc. Am. A* 21(8): 1465–1471.
- Maystre, D. & Nevière, M. (1977). Sur une méthode d'étude théorique quantitative des anomalies de Wood des réseaux de diffraction, application aux anomalies de plasmons, *J. Optics (Paris)* 8: 165–174.
- Maystre, D. & Nieto-Vesperinas, M. (1992). Effects of total internal reflection on the reflectivities of dielectric gratings, *J. Opt. Soc. Am. A* 9(12): 2218–2222.

- Mendes, R., Kennedy, J. & Neves, J. (2004). The fully informed particle swarm: Simpler maybe better, *IEEE Transactions in Evolutionary Computing* 8: 204–210.
- Michalewicz, Z. (1992). *Genetic Algorithms + Data Structure = Evolution Programs*, Springer-Verlag, New York.
- Neff, H., Zong, W., Lima, A., Borre, M. & Holzhüter, G. (2006). Optical properties and instrumental performance of thin gold films near the surface plasmon resonance, *Thin Solid Films* 496: 688–697.
- Raether, H. (1988). *Surface Plasmons on Smooth and Rough Surfaces and on Gratings*, Springer-Verlag, Berlin.
- Schwefel, H. P. (1995). *Evolution and Optimum Seeking*, John Wiley & Sons Inc., New York.
- Shi, Y. & Eberhart, R. C. (1998). A modified particle swarm optimizer, *Proc. IEEE Congress on Evolutionary Computation (CEC'98)*, Anchorage, AK, pp. 69–73.
- Simon, H. J., Mitchell, D. E. & Watson, J. G. (1975). Surface plasmons in silver films - a novel undergraduate experiment, *Am. J. Phys.* 43(7): 630–636.
- Veenhuis, C. (2006). Advanced meta-PSO, *Proc. IEEE Sixth International Conference on Hybrid Intelligent Systems (HIS'06)*, Rio de Janeiro, Brazil, pp. 54–59.
- Whitehead, B. A. & Choate, T. D. (1996). Cooperative-competitive genetic evolution of radial basis function centers and widths for time series prediction, *IEEE Transactions on Neural Networks* 7: 869–880.
- X. Yao, Y. L. & Lin, G. M. (1999). Evolutionary programming made faster, *IEEE Trans. Evol. Comput.* 3: 82–102.
- Yang, J.-M., Chen, Y.-P., Horng, J.-T. & Kao, C.-Y. (1997). Applying family competition to evolution strategies for constrained optimization, *Lecture Notes in Computer Science* 1213: 201–211.
- Zhan, Z.-H., Zhang, J., Li, Y. & Chung, H. S.-H. (2009). Adaptive particle swarm optimization, *IEEE Transactions on Systems, Man, and Cybernetics-Part B: Cybernetics* 39: 1362–1381.
- Zhao, X. (2008). Convergent analysis on evolutionary algorithm with non-uniform mutation, *Evolutionary Computation*, IEEE, pp. 940–944.
- Zhao, X., Gao, X.-S. & Hu, Z.-C. (2007). Evolutionary programming based on non-uniform mutation, *Applied Mathematics and Computation* 192: 1–11.



New Perspectives in Biosensors Technology and Applications

Edited by Prof. Pier Andrea Serra

ISBN 978-953-307-448-1

Hard cover, 448 pages

Publisher InTech

Published online 24, June, 2011

Published in print edition June, 2011

A biosensor is a detecting device that combines a transducer with a biologically sensitive and selective component. Biosensors can measure compounds present in the environment, chemical processes, food and human body at low cost if compared with traditional analytical techniques. This book covers a wide range of aspects and issues related to biosensor technology, bringing together researchers from 12 different countries. The book consists of 20 chapters written by 69 authors and divided in three sections: Biosensors Technology and Materials, Biosensors for Health and Biosensors for Environment and Biosecurity.

How to reference

In order to correctly reference this scholarly work, feel free to copy and paste the following:

Dominique Barchiesi (2011). Numerical Optimization of Plasmonic Biosensors, *New Perspectives in Biosensors Technology and Applications*, Prof. Pier Andrea Serra (Ed.), ISBN: 978-953-307-448-1, InTech, Available from: <http://www.intechopen.com/books/new-perspectives-in-biosensors-technology-and-applications/numerical-optimization-of-plasmonic-biosensors>

INTECH

open science | open minds

InTech Europe

University Campus STeP Ri
Slavka Krautzeka 83/A
51000 Rijeka, Croatia
Phone: +385 (51) 770 447
Fax: +385 (51) 686 166
www.intechopen.com

InTech China

Unit 405, Office Block, Hotel Equatorial Shanghai
No.65, Yan An Road (West), Shanghai, 200040, China
中国上海市延安西路65号上海国际贵都大饭店办公楼405单元
Phone: +86-21-62489820
Fax: +86-21-62489821

© 2011 The Author(s). Licensee IntechOpen. This chapter is distributed under the terms of the [Creative Commons Attribution-NonCommercial-ShareAlike-3.0 License](#), which permits use, distribution and reproduction for non-commercial purposes, provided the original is properly cited and derivative works building on this content are distributed under the same license.